Long-term sorption of lincomycin to biochars: The intertwined roles of pore diffusion and dissolved organic carbon

Cheng-Hua Liu [a, b], Ya-Hui Chuang [a, c], Hui Li [a], Stephen A. Boyd [a], Brian J. Teppen [a], Javier M. Gonzalez [d], Cliff T. Johnston [e], Johannes Lehmann [f], Wei Zhang [a, b, *]

[a] Department of Plant, Soil and Microbial Sciences, Michigan State University, East Lansing, MI, 48824, United States
[b] Environmental Science and Policy Program, Michigan State University, East Lansing, MI, 48824, United States
[c] Department of Soil and Environmental Sciences, National Chung-Hsing University, Taichung, 402, Taiwan
[d] National Soil Erosion Research Lab, Agricultural Research Service, United States Department of Agriculture, West Lafayette, IN, 47907, United States
[e] Department of Agronomy, Purdue University, West Lafayette, IN, 47907, United States
[f] Soil and Crop Sciences Section, School of Integrative Plant Science, Cornell University, Ithaca, NY, 14853, United States

ARTICLE INFO

ABSTRACT

Sequestration of anthropogenic antibiotics by biochars from waters may be a promising strategy to minimize environmental and human health risks of antibiotic resistance. This study investigated the long-term sequestration of lincomycin by 17 slow-pyrolysis biochars using batch sorption experiments during 365 days. Sorption kinetics were well fitted to the Weber-Morris intraparticle diffusion model for all tested biochars with the intraparticle diffusion rate constant (k_{id}) of 25.3–166 $\mu g\,g^{-1}$ day$^{-0.5}$ and intercept constant (C_{id}) of 39.0–339 $\mu g\,g^{-1}$, suggesting that the sorption kinetics were controlled by fast initial sorption and slow pore diffusion. The quasi-equilibrium sorption isotherms became more nonlinear with increasing equilibration time at 1, 7, 30, and 365 days, likely due to increasing abundance of heterogeneous sorption sites in biochars over time. Intriguingly, low-temperature (300 °C) and high-temperature (600 °C) biochars had faster sorption kinetics than intermediate-temperature (400–500 °C) biochars at the long term, which was attributed to greater specific surface area and pore volume of high-temperature biochars and the substantial and continuous release of dissolved organic carbon (DOC) from low-temperature biochars, respectively. DOC release enhanced lincomycin sorption by decreasing biochar particle size and/or increasing the accessibility of sorption sites and pores initially blocked by DOC. Additionally, a large fraction (>75%) of sorbed lincomycin in biochars after a 240-day equilibration could not be extracted by the acetonitrile/methanol extractant. The strong sorption and low extraction recovery demonstrated the great potential of biochars as soil amendments for long-term sequestration of antibiotics in-situ.

© 2019 Elsevier Ltd. All rights reserved.

1. Introduction

Antibiotics are used extensively in livestock industry for therapeutic, preventative, and growth promotion purposes (Kumar et al., 2005; Martinez, 2009; Sarmah et al., 2006). The use of antibiotics in animal feeding operations was 14,622 tons in the United States in 2012 and 84,240 tons in China in 2013 (i.e., the two largest users of antibiotics) (Zhang et al., 2015). Globally, the total consumption of antibiotics in livestock industry was about 131,109 tons in 2013 and was projected to increase to 200,235 tons in 2030 (Van Boeckel et al., 2017). Because the administered antibiotics are often poorly metabolized within animals, a large portion of antibiotics are excreted into manure as parent compounds and metabolites, and released into agricultural soils and waterbodies through manure land applications (Kuchta and Cessna, 2009; Kummerer, 2009; Zhu et al., 2013). The widespread and repeated manure application has increased environmental concentrations of anthropogenic antibiotics, thus raising serious concerns about the proliferation of antibiotic resistant bacteria and associated food safety and human health impacts (Chee-Sanford et al., 2009; Heuer et al., 2011; Martinez, 2009; Rivera-Utrilla et al., 2013). Mitigation strategies to reduce the release, transport, and bioavailability of manure-borne

antibiotics in soils are urgently needed to minimize their environmental risks. Enhancing sequestration of antibiotics from waters in soils by biochar amendment may be a promising strategy for this purpose.

Biochars are carbonaceous porous materials produced from the pyrolysis of biomass under oxygen-limited conditions at a typical temperature range of 300–700 °C (Lehmann and Joseph, 2015). Biochars have been promoted as sorbents and soil amendments for agronomical and environmental applications such as increasing soil carbon storage, improving soil structure and quality, and immobilizing environmental contaminants (Beesley et al., 2011; Lehmann, 2007; Lehmann and Joseph, 2015). Sorption plays an important role in controlling the fate, transport, and bioavailability of antibiotics in soils, and the porous nature and heterogeneous surfaces of biochars lead to an excellent sorption ability for antibiotics (Ahmed et al., 2015; Kah et al., 2017; Peiris et al., 2017). The interactions between antibiotics and biochars may be controlled by hydrophobic partitioning, van der Waals forces, hydrogen (H) bonding, charge-assisted H bonding (CAHB), π-π electron donor–acceptor (EDA) interaction, electrostatic interaction, and pore filling (Ahmed et al., 2015; Kah et al., 2017; Peiris et al., 2017). The relative contribution of each sorption mechanism is collectively determined by physicochemical properties of antibiotics (e.g., hydrophobicity, polarity, ionization, and molecular structure) and biochars (e.g., surface area, surface charge, surface functionalization, and pore structure) as well as environmental factors (e.g., pH, ionic strength, and co-solutes) (Kah et al., 2017; Peiris et al., 2017). Thus, studies on contaminant sorption to biochars have recently focused on clarifying the complexity in sorption processes and controlling factors.

Pyrolysis temperature is one of the key factors determining physicochemical and sorption properties of biochars (Ahmad et al., 2014; Beesley et al., 2011; Lian and Xing, 2017; Tan et al., 2015). With increasing pyrolysis temperature, surface area and pore volume of biochars increase, but densities of oxygen-containing (e.g., carboxyl and hydroxyl groups) and aliphatic (e.g. methyl group) functional groups decrease with a concomitant increase in aromaticity (Chen et al., 2012; Keiluweit et al., 2010; Lian and Xing, 2017). Due to larger surface area and porosity of high-temperature biochars, they often had stronger sorption affinity to antibiotics such as ciprofloxacin (Shang et al., 2016), norfloxacin (Feng et al., 2015), tetracycline (Huang et al., 2017; Wang et al., 2017b), and sulfamethoxazole (Pan et al., 2012; Wu et al., 2013; Zheng et al., 2013) than lower-temperature biochars. However, a number of studies reported the absence or opposite of such trend with regard to pyrolysis temperature for the sorption of ofloxacin (Wu et al., 2013), norfloxacin (Wu et al., 2013), and sulfamethoxazole (Lian et al., 2014) to biochars. Clearly, the effect of pyrolysis temperature on physicochemical properties of biochars and sorption of antibiotics to biochars has yet to be fully understood.

Additionally, considering the heterogeneous nature of biochar pore structures, sorption of antibiotics may need a longer time to reach a true equilibrium. Kasozi et al. (2010) reported that the sorption kinetics of catechol on biochars reached equilibrium after 14 days. Chen et al. (2012) found that the sorption of naphthalene to biochars could take up to 36 days to reach equilibrium, depending on pyrolysis temperature of biochars. Our previous study showed that lincomycin sorption to biochars quickly reached a quasi-equilibrium in about 2 days, but did not reach the true equilibrium even after 180 days (Liu et al., 2016). For most antibiotics that have been studied, the reported sorption equilibration time with biochars was generally varied from several hours to a few days (Feng et al., 2015; Huang et al., 2017; Lian et al., 2014; Pan et al., 2012; Shang et al., 2016; Wang et al., 2017b; Wu et al., 2013; Zheng et al., 2013). Thus, some of those sorption experiments may have only reached a quasi-equilibrium during such an equilibration

time that may be too short for certain antibiotics considering their ongoing sorption over the long term. Consequently, the contribution of pore diffusion to the overall sorption may be underestimated due to short equilibration times. Furthermore, biochars could release a substantial amount of dissolved organic carbon (DOC, including truly dissolved and colloidal DOC) upon exposure to water (Lin et al., 2012; Mukherjee and Zimmerman, 2013; Qu et al., 2016; Smith et al., 2016; Zimmerman and Gao, 2013), which may change the biochar surface and pore structure. For example, these water-soluble organic compounds (i.e., DOC) may initially fill up the biochar pores during pyrolysis, or adsorb on the biochar surface, thus blocking the sorptive sites for organic contaminants (Wang et al., 2017a). The released DOC from biochars (hereafter denoted as biochar-DOC) may enhance the sorption of antibiotics to biochars. However, the effect of long-term DOC release from biochars on their sorption capacity for antibiotics has not been well studied.

Therefore, this study aimed to examine: (1) the long-term sequestration of antibiotics by biochars and (2) the effect of the long-term biochar-DOC release on the sorption of antibiotics to biochars. Lincomycin was selected in this study because it is one of the most widely used antibiotics in food animal production, and is also medically important in human therapy (Van Epps and Blaney, 2016; Zhang et al., 2015). Lincomycin is relatively resistant to environmental degradation (Andreozzi et al., 2006; Loftin et al., 2008) and has been frequently detected in soil and water (Kolpin et al., 2002; Watanabe et al., 2010). The long-term sorption kinetics and isotherms of lincomycin by 17 slow-pyrolysis biochars prepared from 7 manure feedstocks at 300–600 °C and one wood feedstock at 500 °C were evaluated to elucidate the underlying sorption mechanisms along with the release of biochar-DOC. The applied initial concentrations of lincomycin were in the range of 100–1000 $\mu g\,L^{-1}$, which have been detected in livestock wastewaters (Sim et al., 2011; Zhang et al., 2018). In addition, a commercial graphite powder was selected to represent the sorption of lincomycin on nonporous carbonaceous sorbents as compared to porous biochars.

2. Materials and methods

2.1. Chemicals

Lincomycin hydrochloride ($\geq$90%) and sodium azide (NaN$_3$, $\geq$99.5%) were purchased from Sigma-Aldrich (St. Louis, MO, USA), and sodium chloride (NaCl), sodium bicarbonate (NaHCO$_3$), sodium carbonate (NaCO$_3$) and sodium hydroxide (NaOH) from J.T. Baker (Phillipsburg, NJ, USA). Selected physicochemical properties of lincomycin are provided in Table S1 of Supplementary Material. All chemical reagents used were of analytical grade. Deionized (DI) water from a Milli-Q water system (Millipore, Burlington, MA, USA) was used for preparing all aqueous solutions.

2.2. Sorbents

Sixteen manure-based biochars and one wood-based biochar were produced by Best Energies Inc. (Daisy Reactor, Cashton, WI, USA). The feedstocks and production conditions of these biochars have been described in detail elsewhere (Enders et al., 2012; Rajkovich et al., 2011). Briefly, the feedstocks were bull manure with sawdust bedding (BM), dairy manure with rice hull bedding (DM), poultry manure with sawdust bedding (PM), raw dairy manure (RDM), digested dairy manure (DDM), composted digested dairy manure (CDM), composted digested dairy manure mixed with woodchip waste in a 1:1 ratio (CDMW), and woodchip waste (WW). The same source of dairy manure was used to produce RDM,

DDM, CDM, and CDMW with different pretreatments before pyrolysis in a Daisy Reactor at BEST Energies Inc. The feedstocks were slowly pyrolyzed in a N_2 atmosphere at 300, 400, 500 or 600 °C with a heating rate of <10 °C min^{-1} and a retention time of 15—20 min. The produced biochars were ground and sieved to obtain particles in the 75—150 μm size fraction, and then stored in glass vials prior to use. The fine particle size fraction of biochars was selected because biochars had a wide particle size distribution ranging from submicrons to centimeters (IBI, 2019; Lehmann and Joseph, 2015) and finer biochar particles have greater potential to sequester antibiotics in the environment (Liu et al., 2016). These biochars were hereafter labeled using feedstock abbreviation and pyrolysis temperature, e.g., BM300 for bull manure with sawdust bedding pyrolyzed at 300 °C. Nonporous graphite powder (<150 μm, 99.9% C) was purchased from Sigma-Aldrich and used as received.

2.3. Sorbent characterization

The proximate (volatile matter, fixed carbon, and ash), ultimate (C, H, O, and N), and total elemental (P, K, S, Ca, Mg, Na, Fe, Mn, Zn, and Si) analyses of the biochars have been performed and reported previously (Enders et al., 2012; Rajkovich et al., 2011). Specific surface area (SSA) and micropore volume (V_{mic}) of the biochars were measured by CO_2 adsorption by a Tristar II 3020 analyzer (Micromeritics, Norcross, GA, USA) at Pacific Surface Science Inc. (Oxnard, CA, USA). Detailed pore size distribution was not determined in this study because the porosity of biochars can be changed during degassing (Sigmund et al., 2017), especially for poorly-carbonized biochars (see Supplementary Material S1 for detail). Zeta potential of the biochar particles was determined by a Zetasizer Nano-ZS (Malvern Instruments, Malvern, Worcestershire, UK) for biochar suspensions prepared according to the procedure described in Supplementary Material S1. Additionally, BM300 and BM600 were selected as model biochars (representing poorly- and highly-carbonized biochars, respectively) for further studying the characteristics of biochar particles after water exposure. The shape and surface morphology of BM300 and BM600 particles before and after 1-d and 365-d kinetic sorption experiments (described later) and 1-d exposure to 0.1 M NaOH solution (as described in Supplementary Material S1) were investigated with a JSM-7500 F scanning electron microscope (SEM) (JEOL, Akishima, Tokyo, Japan). The particle size distribution of BM300 and BM600 particles in suspensions was determined by dynamic light scattering method using the Zetasizer.

2.4. Sorption experiments

Batch sorption experiments were conducted in amber borosilicate glass vials with polytetrafluoroethylene (PTFE) lined screw-caps (Kimble, Vineland, NJ, USA). All vials were covered with aluminum foils to prevent any potential photodegradation of lincomycin. The lincomycin solutions were freshly prepared in DI water with ionic strength of 0.02 M and pH of 10 using background electrolytes of 6.7 mM NaCl, 2.5 mM Na_2CO_3, and 2.5 mM $NaHCO_3$. A biocide NaN_3 of 200 mg L^{-1} was included to prevent any biodegradation of lincomycin during the long-term sorption experiments. As nonelectrostatic sorption (free of solution pH and ionic strength effect) is more useful for estimating lincomycin sequestration capacity of biochars, this study used solution pH of 10 at which lincomycin is neutral and mainly reacts with biochar surfaces via nonelectrostatic interactions (Liu et al., 2016). All sorption experiments were performed in duplicate at room temperature (23 ± 1 °C) and a sorbent-water ratio of 1 g L^{-1}. The above experimental condition and setup for the batch sorption studies

were followed unless noted otherwise.

For the kinetic sorption experiments, 8 mg of each sorbent were mixed with 8 mL of 1000 μg L^{-1} lincomycin in 8-mL vials and then agitated on an end-over-end shaker (Glas-Col, Terre Haute, IN, USA) at 30 rpm in dark for the duration of 1—365 days. At predetermined time intervals, two vials for each sorbent were retrieved from the shaker. The vials were centrifuged at $2430 \times g$ for 20 min at room temperature, and the top 2 mL of supernatants were collected and filtered through a 0.45-μm mixed cellulose esters syringe filter (Millipore, Burlington, MA, USA). The first 1-mL filtrate was discarded, and the following 1-mL filtrate was collected to minimize the potential loss of lincomycin sorbed by the filter. The concentrations of lincomycin in the filtrate was determined by a Shimadzu Prominence high-performance liquid chromatograph (Columbia, MD, USA) coupled to an Applied Biosystems Sciex 3200 triple quadrupole mass spectrometer (Foster City, CA, USA) (LC-MS/MS) (Chuang et al., 2015). In agreement with our previous study (Liu et al., 2016), the sorbent-free control experiments showed a negligible loss of lincomycin during the experiments (Fig. S1), and there were no degradation products (Calza et al., 2012) detected in the filtrates of sorbent-free control experiments (BM300 and BM600) at day 365 using precursor ion scan mode by the tandem mass spectrometry. Therefore, the difference between the initial and final solution concentrations was used to calculate the sorbed lincomycin concentration in the sorbents. In addition, the DOC in the filtrate is operationally defined as biochar-DOC in this study. Because the filtrate volume was small, and if diluted, the biochar-DOC concentration could be below the detection limit of total organic carbon analyzer, the concentration of biochar-DOC in the filtrate was determined by ultraviolet (UV) absorption at 254 nm and E_2/E_3 ratio (the ratio of absorbance at 254 nm over absorbance at 365 nm) on a Varian Cary 50 Bio UV—visible spectrophotometer (Varian, Palo Alto, CA, USA), using our recently developed method (Liu et al., 2019). Details of the LC-MS/MS and UV analytical protocols are provided in Supplementary Material. The solution pH generally remained unchanged (i.e., pH = 10 ± 0.1) during the long-term sorption experiments for biochars. However, in the experiments with BM300, DM300, PM00, and DDM500 solution pH decreased to 9.1 ± 0.3 after 365 days presumably due to the greater amount of biochar-DOC released into solution. This study at pH of 10 is considered relevant to field soils because it may simulate the magnitude of DOC release from biochars over a long period (years), thus allowing for assessing sorption properties of aged biochars in alkaline soils.

To conduct the quasi-equilibrium sorption isotherms, 8 mg of each sorbent were mixed with 8 mL lincomycin solutions with a series of initial concentrations ranging from 100 to 1000 μg L^{-1}. The suspensions were shaken end-over-end at 30 rpm in dark. At 1 day, 1 week (7 days), 1 month (30 days), and 1 year (365 days), the vials were retrieved, centrifuged, filtered, and determined for the lincomycin concentration by the LC-MS/MS as described previously.

2.5. Effects of biochar-DOC on lincomycin sorption

To further elucidate the role of biochar-DOC on the sorption of lincomycin to biochars, three additional experiments were performed as detailed in Supplementary Material S1. First, the freely dissolved lincomycin and DOC-bound lincomycin in solutions were determined using the solid-phase extraction method (Ding et al., 2013). This experiment was performed for the DOC concentration of 186, 93.8, 97.4, and 89.6 mg-C L^{-1} extracted from BM300, DM300, PM300, and DDM500, respectively. Its results could allow us to evaluate the contribution of lincomycin bound with biochar-DOC to total lincomycin sorption and determine if the enhanced

lincomycin sorption over time was due to the binding of lincomycin with biochar-DOC. Second, the lincomycin sorption to a wood biochar (WW500) was measured in the absence and the presence of biochar-DOC at 17.2, 7.94, 11.1, and 10.9 mg-C L^{-1} extracted from BM300, DM300, PM300, and DDM500, respectively. The control experiments without WW500 were also performed, and the lincomycin concentrations in solution had no significant difference regardless of the presence of biochar-DOC during 60 days (data not shown). This experiment allowed us to evaluate the effect of free biochar-DOC in solution on lincomycin sorption to biochars. Finally, to evaluate the change in the lincomycin sorption to biochars after the DOC release, each BM300, DM300, PM300, DDM500, and BM600 biochar was mixed with DI water for 40 days or with 0.1 M NaOH for 1 day (only for BM300, BM600, and DM300), respectively. The washed biochars were then separated from the washing solutions, further rinsed with DI water to remove any remaining DOC and salts, and freeze-dried before being used in the kinetic sorption experiments as described earlier. Washing with DI water removed 20.7, 10.4, 10.8, 9.92, and 0.18 mg-C/g-biochar of DOC from BM300, DM300, PM300, DDM500, and BM600 biochars, whereas 105, 75.2, and 3.37 mg-C/g-biochar of DOC were removed from BM300, DM300, and BM600 biochars by 0.1 M NaOH, respectively.

2.6. Extraction of sorbed-lincomycin from biochars

Single-point batch extraction experiments were performed to test the extraction recovery of sorbed lincomycin on the biochars. The sorbed lincomycin on the biochars after 240-day sorption equilibration was extracted using the ultrasonic-assisted solvent extraction with an acetonitrile/methanol mixture (8/2 by volume), as described in Supplementary Material S1.

2.7. Mathematical modeling

The experimental sorption kinetics were fitted to the Weber-Morris intraparticle diffusion model (Weber and Morris, 1963; Wu et al., 2009):

$$q_t = k_{id}t^{0.5} + C_{id} \tag{1}$$

where q_t (μg g^{-1}) is the sorbed lincomycin concentration in the solid phase at time t, k_{id} (μg g^{-1} day$^{-0.5}$) is the intraparticle diffusion rate constant, t (day) is the reaction time, and C_{id} (μg g^{-1}) is the intercept constant that reflects the contribution from the rapid initial sorption (Wu et al., 2009). At the final stage of several kinetic sorption experiments, lincomycin concentrations in solution became either minimal or non-detectable, resulting in decreased intraparticle diffusion rate (Wu et al., 2001) and inaccurate sorption measurement, respectively. Thus, the sorption data collected during those periods were excluded from the fitting.

According to Wu et al. (2009), the relative importance of intraparticle diffusion and initial sorption could be further analyzed based on following equations:

$$\left(\frac{q_t}{q_{ref}}\right) = 1 - R_{id}\left[1 - \left(\frac{t}{t_{ref}}\right)^{0.5}\right] \tag{2}$$

$$R_{id} = \frac{k_{id}t_{ref}^{0.5}}{q_{ref}} \tag{3}$$

where t_{ref} (day) is the longest time used when fitting the intraparticle diffusion model, q_{ref} (μg g^{-1}) is the sorbed lincomycin concentration in the solid phase at time t_{ref}, and R_{id} is the intraparticle diffusion factor that represents the relative contribution of the intraparticle diffusion to the total sorption.

The quasi-equilibrium sorption isotherms were fitted nonlinearly to the Freundlich model (Xing and Pignatello, 1996):

$$q_t = K_F C_t^N \tag{4}$$

where q_t (μg g^{-1}) is the sorbed lincomycin concentration in the solid phase at time t, C_t (μg L^{-1}) is the lincomycin concentration in the solution at time t, K_F (μg^{1-N} g^{-1} L^N) is the Freundlich sorption coefficient, and N (dimensionless) is the Freundlich nonlinearity factor. Assuming multiple sorption sites on sorbent surface, mathematically it has been proven that decreasing in N value suggests an increase in sorption site heterogeneity (Sposito, 1980).

Because K_F values could not be compared directly unless N is the same, sorption distribution coefficient was calculated for comparison of lincomycin sorption by biochars:

$$K_d = \frac{q}{C_w} = K_F C_w^{N-1} \tag{5}$$

where K_d (L g^{-1}) is the sorption distribution coefficient, q (μg g^{-1}) is the sorbed lincomycin concentration in the solid phase and C_w (μg L^{-1}) is the dissolved lincomycin concentration in the solution phase.

The data fitting and statistical analysis were performed with Mathworks MATLAB R2016a Curve Fitting Toolbox (Natick, MA, USA) and IBM SPSS Statistics 25 (Armonk, NY, USA), respectively. The goodness of fit was evaluated using the coefficient of determination (R^2) and the root mean squared error (RMSE). Significant differences between experimental treatments were analyzed using one-way ANOVA with post-hoc Tukey test (p-value < 0.05).

3. Results and discussion

3.1. Characterization of biochars

The selected physicochemical properties of 17 tested slow-pyrolysis biochars are shown in Table S2 in Supplementary Material. The effect of pyrolysis temperature on physicochemical properties of tested biochars was generally consistent with previous findings (Chen et al., 2008; Keiluweit et al., 2010), except for PM biochars due to their higher ash content (Table S2 and Fig. S2). Volatile matter content (25.7–55.5%) decreased, whereas fixed carbon content (0–62.1%) and ash content (7.7–58.5%) increased with increasing pyrolysis temperature, due to increased carbonization of biomass at higher pyrolysis temperature (Antal and Gronli, 2003; Keiluweit et al., 2010). The volatile matter and fixed carbon contents could approximate the easily mineralizable and persistent fractions of biochars, respectively (Keiluweit et al., 2010). In addition, the biochars produced from PM, CDM, and CDMW had a greater ash content (32.0–55.8%) than that from BM, DM, DDM, and WW (7.70–18.8%), which was attributed to mineral content in their feedstock (Bernal et al., 2009). For biochars from the same feedstocks, total C content (27.8–85.9%) increased, while total O (11.6–26.6%), H (0.4–4.9%), and N (0.4–2.6%) contents decreased with increasing pyrolysis temperature. Accordingly, atomic ratios of H/C (0.17–0.97) and (O + N)/C (0.13–0.52) decreased at higher pyrolysis temperature, suggesting that high-temperature biochars had more condensed aromatic structures and less polar functional groups (Chen et al., 2008; Chun et al., 2004; Keiluweit et al., 2010). SSA (45.0–271 m^2 g^{-1}) and V_{mic} (0.02–0.12 cm^3 g^{-1}) of the tested biochars generally increased with increasing pyrolysis temperature. SEM images of BM300 and BM600 revealed that biochar pores were irregular in shape and heterogeneous in pore size from

nanometers to micrometers (Fig. S3). Finally, zeta potential of tested biochars ranged from −64 to −43 mV at solution pH of 10 and ionic strength of 0.02 M (Table S2), indicating that the biochars carried net negative surface charge under the experimental conditions.

3.2. Long-term sorption kinetics

As shown in Fig. 1 and Fig. S1, lincomycin sorption onto the biochars occurred rapidly in the initial sorption phase (within the first day), followed by a slower sorption over the long term (up to 365 days). For all biochars, the long-term lincomycin sorption did not fully occupy all the sorption sites in the biochars (i.e., reaching sorption saturation), and continuously increased towards a point when dissolved lincomycin concentration in solution became minimal or non-detectable (defined as apparent sorption equilibrium here). The lincomycin sorption kinetics approached an apparent sorption equilibrium within 365 days for most biochars (except for BM500, PM400, PM500, and CDM500). Approximately 7–34% of initially applied lincomycin was removed by the biochars after 1 day, whereas up to 83–100% of that was removed by 365 days, except for PM400 (54%). Considering the porous nature of biochars, the fast initial sorption was primarily attributed to the instantaneous or very rapid sorption on the external surface of biochars that provides readily accessible sorption sites for lincomycin. The subsequent long-term slow sorption was mainly caused by the relatively slower intraparticle diffusion into the internal biochar pore structures that provide abundant sorption sites, but require longer time for lincomycin to access. As lincomycin is relatively bulky, non-aromatic, and flexible in its molecular structure (Table S1), its diffusion into the irregularly-shaped biochar pores might be prolonged. As a comparison, the sorption of lincomycin onto the nonporous graphite reached a sorption equilibrium within 1 day and remained unchanged for 30 days due to the lack of pore structures (Fig. S4). The significant difference in the sorption behaviors between the porous biochars and the nonporous graphite further supported that the sorption of lincomycin to the biochars was controlled by fast surface sorption in the short term and slow intraparticle diffusion in the long term.

The tested biochars had different sorption kinetics depending on the pyrolysis temperature and feedstock, presumably due to the heterogeneity in their pore structures and surface chemistries. Overall, the sorption kinetics decreased in the order: BM300 > BM400 ≈ BM600 > BM500 (Fig. 1a), DM300 ≈ DM600 > DM400 (Fig. 1b), and PM600 > PM300 > PM500 > PM400 (Fig. 1c) and DDM500 > DDM600 ≈ RDW500 > WW500 > CDMW500 > CDM500 (Fig. 1d). Specifically, the biochars produced at the lowest and highest pyrolysis temperature (i.e., 300 and 600 °C) generally had faster sorption kinetics and reached the apparent equilibrium more quickly than the biochars produced at intermediate pyrolysis temperature (i.e., 400–500 °C). The sorption kinetics prior to the apparent sorption equilibrium were well fitted by the Weber-Morris
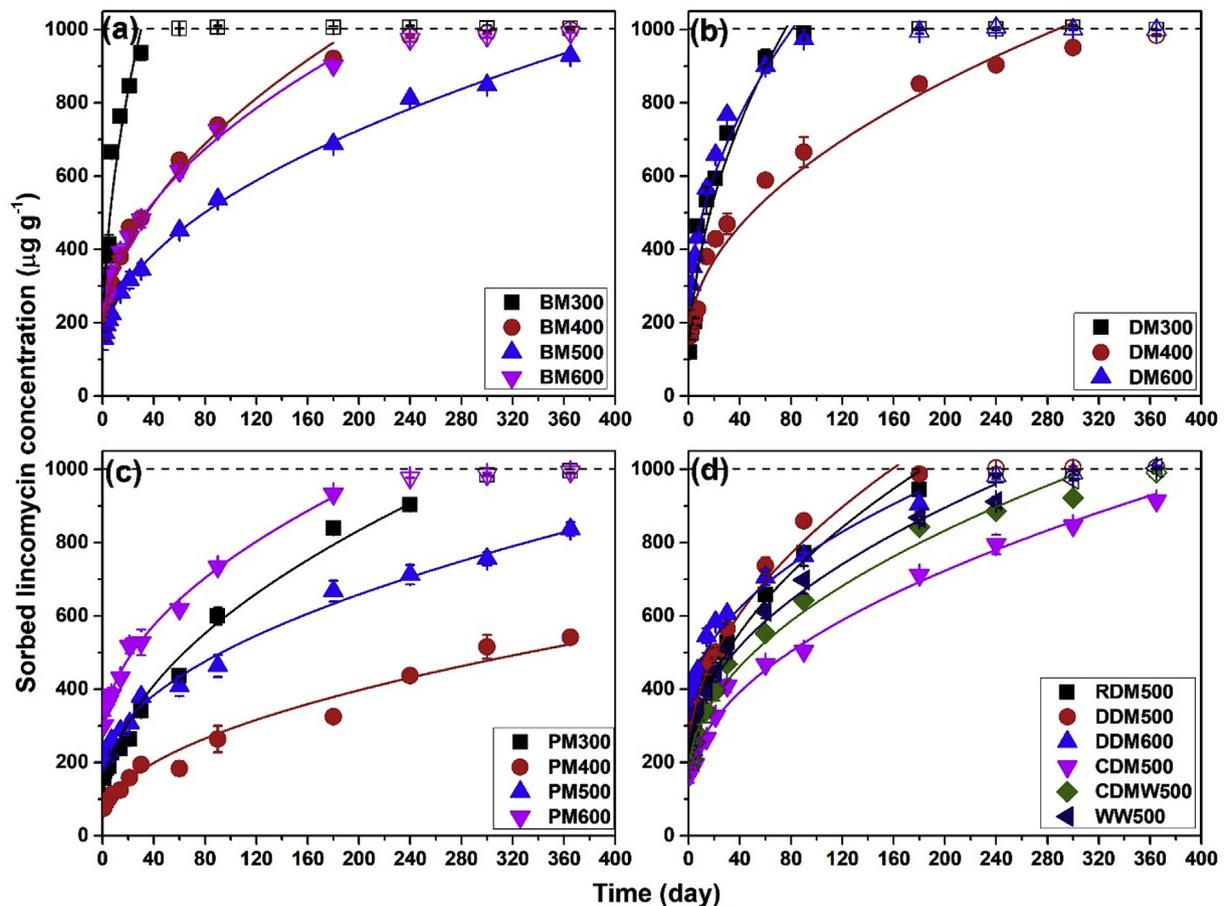
Fig. 1. Long-term kinetics of lincomycin sorption by biochars: (a) bull manure with sawdust bedding (BM), (b) dairy manure with rice hull bedding (DM), (c) poultry manure with sawdust bedding (PM), and (d) raw dairy manure (RDM), digested dairy manure (DDM), composted digested dairy manure (CDM), composted digested dairy manure mixed with woodchip waste in a 1:1 ratio (CDMW), and woodchip waste (WW). The sorption data were fitted by the intraparticle diffusion model (solid line), and the hollow data were excluded from the fitting due to approaching apparent sorption equilibrium (dash line). The symbols and error bars represent mean and standard deviation of duplicates.

intraparticle diffusion model for all tested biochars (Table S3). The k_{id} and C_{id} values were in the range of 25.3–166 μg g^{-1} day$^{-0.5}$ and 39.0–339 μg g^{-1}, respectively.

Interestingly, the C_{id} values showed a positive linear relationship (Fig. 2b), while the k_{id} values exhibited a U-shaped relationship with increasing pyrolysis temperature from 300 to 600 °C (Fig. 2a). For example, the average C_{id} values increased monotonically from 70.9 ± 18.7 μg g^{-1}, 107 ± 59 μg g^{-1} and 164 ± 37 μg g^{-1} to 247 ± 71 μg g^{-1}, whereas the k_{id} values followed the order of 300 °C (110 ± 56 μg g^{-1} day$^{-0.5}$) > 600 °C (59.5 ± 19.8 μg g^{-1} day$^{-0.5}$) > 500 °C (48.8 ± 10.3 μg g^{-1} day$^{-0.5}$) ≈ 400 °C (45.8 ± 18.6 μg g^{-1} day$^{-0.5}$) for the biochars produced at 300, 400, 500, 600 °C, respectively. As the C_{id} values represent the initial surface sorption, this positive linear trend was expected because of the greater external surface area of higher-temperature biochars than that of lower-temperature biochars. Furthermore, the observed U-shaped relationship between k_{id} and pyrolysis temperature was unique, which cannot be explained by any measured physicochemical properties of biochars. The greater k_{id} of the higher-temperature biochars might result from their greater SSA and V_{mic} (Table S2). However, the greater k_{id} for the lower-temperature (300 °C) biochars may be controlled by different mechanisms as elucidated later.

The R_{id} values reflect the relative contribution of initial sorption and intraparticle diffusion to the total sorption (Wu et al., 2009).
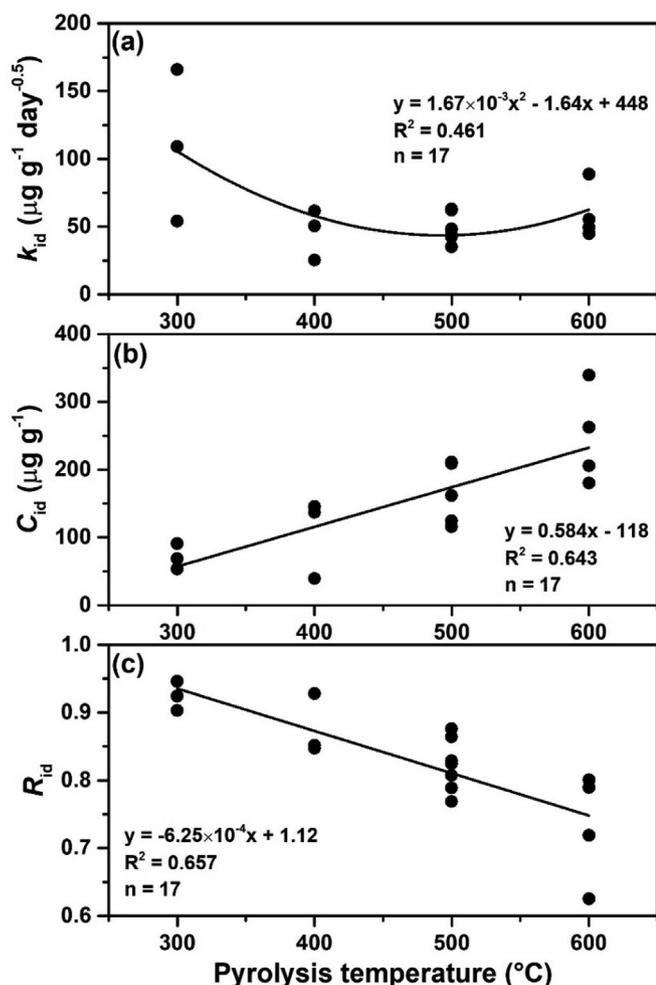

Fig. 2. The relationship of (a) intraparticle diffusion rate constant (k_{id}), (b) initial sorption (C_{id}), and (c) interparticle diffusion factor (R_{id}) versus pyrolysis temperature for 17 biochars.

The R_{id} values closer to one indicate a dominant contribution from the intraparticle diffusion, whereas the R_{id} values closer to zero imply a primary contribution of initial sorption. According to Wu et al. (2009), the lincomycin sorption kinetics of BM300, DM300, PM300, and PM400 can be classified as a weak initial sorption and strong intraparticle diffusion ($1.0 > R_{id} > 0.9$). For the rest of the biochars produced at 400, 500, and 600 °C, the lincomycin sorption kinetics can be classified as intermediate initial sorption and intraparticle diffusion ($0.9 > R_{id} > 0.5$). The R_{id} of all tested biochars ranged from 0.625 to 0.946, showing a negative correlation with pyrolysis temperature (Fig. 2c). Thus, the relative contribution of initial sorption was more pronounced for the high-temperature biochars, presumably due to their greater SSA (Table S2).

As lincomycin exists as neutral species (~100%, pKa = 7.6) in aqueous solution under experimental pH of 10, is very hydrophilic, and lacks π-electron donor or acceptor moieties (Table S1), lincomycin sorption to biochars was unlikely due to hydrophobic partition, electrostatic and π-π EDA interactions (Liu et al., 2016). Therefore, H-bonding, van der Waals forces, and pore diffusion could reasonably be considered as possible mechanisms contributing to lincomycin sorption on biochars (Liu et al., 2016). Because lower-temperature biochars contained more oxygen-containing functional groups and lower SSA and micropore volume than higher-temperature biochars, the contribution of H-bonding may be more important for lincomycin sorption to the low-temperature biochars, whereas the van der Waals interaction may be more important for the high-temperature biochars. However, the different relative contribution of H-bonding and van der Waals interactions in lincomycin sorption still cannot explain why the greater k_{id} values were observed for the low-temperature biochars than for the intermediate-temperature biochars.

To further examine possible mechanisms for the above observation, we hypothesized that the release of DOC from biochars may play an important role in lincomycin sorption by biochars. The long-term release kinetics of DOC from the tested biochars showed that the lower-temperature biochars (300–400 °C) generally had greater release of DOC than the higher-temperature biochars (500–600 °C) except for DDM500 and DDM600 (Fig. S5). The leachable biochar-DOC concentrations increased with decreasing pyrolysis temperature due to the greater labile carbon fraction in the lower-temperature biochars (Fig. S6a). In addition, the released DOC from the lower-temperature biochars generally had higher molecular weight (as indicated by lower E_2/E_3 ratios) (De Haan and De Boer, 1987; Uyguner and Bekbolet, 2005) than higher-temperature biochars (Fig. S6b). Thus, the continual and significant release of DOC from lower-temperature biochars probably enhanced their lincomycin sorption during the long-term sorption. To further investigate the observed enhancement of lincomycin sorption to the biochars of higher DOC concentration, more experiments were performed as discussed later.

3.3. Long-term sorption isotherms

The quasi-equilibrium isotherms of lincomycin to the 17 biochars with contact time of 1, 7, 30, and 365 days were all nonlinear and exhibited a concave-downward shape (Fig. 3 and Fig. S7). All quasi-equilibrium isotherm data could be fitted reasonably well to the Freundlich model ($R^2 = 0.791$–0.978 and RMSE = 6.21–92.6 μg g^{-1}, Table S4). The K_d values were then calculated from the fitted Freundlich parameters at $C_w = 1$ μg L^{-1} (Table S4). As expected, for all biochars the K_d values increased, but the N values decreased with increasing equilibration time. For example, the N values decreased from 0.727 after 1 day to 0.424 after 30 days for BM300 and from 0.510 after 1 day to 0.325 after 365 days for BM600 (Fig. 3a and d). The lower N values (i.e., more nonlinear) observed at the longer
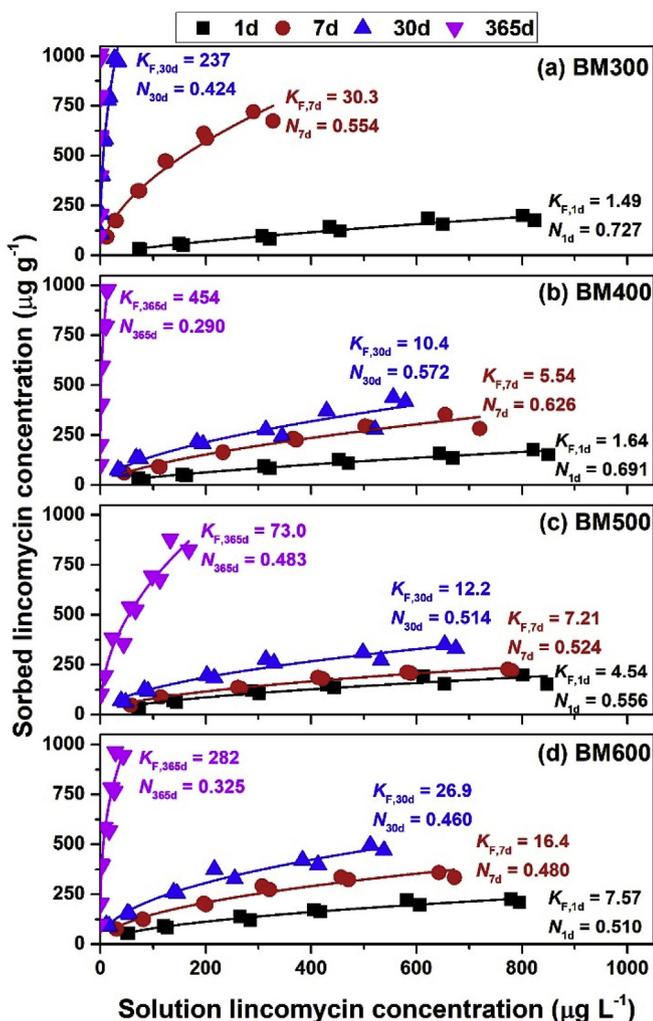
Fig. 3. Quasi-equilibrium sorption isotherms of lincomycin by bull manure-based biochars at 1, 7, 30, and 365 days: (a) BM300, (b) BM400, (c) BM500, and (d) BM600. The isotherms were fitted by the Freundlich model (solid line). K_F (μg^{1-N} g^{-1} L^N) is the Freundlich sorption coefficient, and N (dimensionless) is the Freundlich nonlinearity factor.

equilibration time might suggest a more heterogeneous energy distribution of the sorption sites in the biochars (Sposito, 1980), which could be explained by the greater contribution of intra-particle pore diffusion allowing lincomycin molecules to interact with more heterogeneous pore space and sorptive sites (Pignatello, 2013). It should be noted that this interpretation was based on mathematical fitting of the sorption isotherms, and more direct evidence on lincomycin interaction with surface sorption sites is needed in the future. As a comparison, the sorption isotherms of lincomycin for the nonporous graphite after 1 day and 30 days were almost identical with similar K_d and N values due to the absence of intraparticle diffusion (Fig. S4b). This result further confirmed that the observed time-dependent lincomycin sorption isotherms were caused by increasing contribution of intraparticle diffusion.

Similar to the kinetic sorption data, there was an equilibration-time-dependent relationship between K_d or N values and pyrolysis temperature (Table S4 and Fig. S8). The K_d values exhibited a positive linear relationship with pyrolysis temperature increasing from 300 to 600 °C for the equilibration time after 1 day, but gradually became the U-shaped relationship as the equilibration time extended to 7 and 30 days (Fig. S8a). The N values exhibited a

negative linear relationship with increasing pyrolysis temperature from 300 to 600 °C for the equilibration time after 1 day, but again gradually became an inverted U-shaped relationship as the equilibration time increased to 7 and 30 days (Fig. S8b). The positive and negative linear relationship for K_d and N with pyrolysis temperature after 1 day suggests that the lincomycin sorption to biochars became greater and more nonlinear at higher pyrolysis temperature, presumably due to greater SSA and wider sorption site energy distribution on highly-carbonized carbon domain for higher-temperature (i.e., 600 °C) biochar (Zhang et al., 2011). Interestingly, at the longer equilibration time, the lower-temperature (i.e. 300 °C) biochar had greater sorption affinity and nonlinearity, likely resulting from enhanced intraparticle pore diffusion facilitated by the increasing release of biochar-DOC.

3.4. Effects of biochar-DOC on sorption

We first hypothesized that lincomycin might bind with the biochar-DOC in solution. If so, lincomycin sorption to biochars could be overestimated when the DOC-bound lincomycin was included into the lincomycin sorption to biochars. At the initial lincomycin concentration of 1000 $\mu g\,L^{-1}$, 15, 6.0, 5.8, and 3.0% of initially applied lincomycin was bound to DOC-BM300, DOC-DM300, DOC-PM300, and DOC-DDM500 of 186, 93.8, 97.4, and 89.6 mg-C L^{-1}, respectively. The distribution coefficients of lincomycin to DOC-BM300, DOC-DM300, DOC-PM300, and DOC-DDM500 were 955, 686, 631, and 348 L kg-C^{-1}, respectively. Based on the biochar-DOC release kinetics (Fig. S5), the biochar-DOC concentrations from day 1 to day 365 in the kinetic sorption experiments were 10.5–84.1, 6.35–51.9, 17.2–41.6, and 10.0–54.9 mg-C L^{-1} for BM300, DM300, PM300, and DDM500, respectively. Even assuming all released biochar-DOC could bind with lincomycin in solution, the fraction of the DOC-bound lincomycin was only 0.9–6.8%, 0.4–3.3%, 1.0–2.5%, and 0.3–1.9% of the initially applied amount for DOC-BM300, DOC-DM300, DOC-PM300, and DOC-DDM500, respectively. Therefore, the contribution of lincomycin sorption to biochar-DOC in solution could not explain the enhanced lincomycin sorption to biochars over time.

Secondly, we hypothesized that the biochar-DOC as co-solute in solution might facilitate the lincomycin sorption to biochars. However, the presence of biochar-DOC as co-solute inhibited the lincomycin sorption onto WW500 (Fig. S9). Compared with lincomycin sorption kinetics without biochar-DOC, the fitted k_{id} value decreased from 55.2 to 13.3–29.1 $\mu g\,g^{-1}$ $day^{-0.5}$ and the fitted C_{id} value decreased from 178 to 70.5–85.6 $\mu g\,g^{-1}$ in the presence of DOC (Table S5). The extent of sorption suppression followed the order of DOC-BM300 ≈ DOC-PM300 > DOC-DM300 > DOC-DDM500, which generally (but not completely) agreed with the DOC concentration trend (DOC-BM300 > DOC-DM300 > DOC-DDM500 > DOC-PM300). Thus, the inhibitory effect of biochar-DOC in solution depends on not only the concentration, but also the chemical composition of biochar-DOC. The observed slower diffusion rate and lower initial sorption confirmed that the biochar-DOC could not enhance the lincomycin sorption by itself. On the contrary, the biochar-DOC in solution strongly suppressed the lincomycin sorption by blocking the pore entrances (i.e., decreased k_{id}) and/or by competing for the external surface sorption sites (i.e., decreased C_{id}) in biochars.

We finally tested the hypothesis that the long-term release of biochar-DOC might gradually increase the accessibility of sorption sites on the external surface and in the biochar pore structure, thus enhancing their sorption for lincomycin. Therefore, the sorption kinetics of lincomycin by raw, DI-washed, and NaOH-washed biochars (selected BM300, DM300, PM300, DDM500, BM600) were analyzed (Fig. 4, Fig. S10 and Table S6). Apparently, the removal of DOC from the biochars (BM300, DM300, PM300, and DDM500) substantially enhanced the lincomycin sorption kinetics (Fig. 4 and
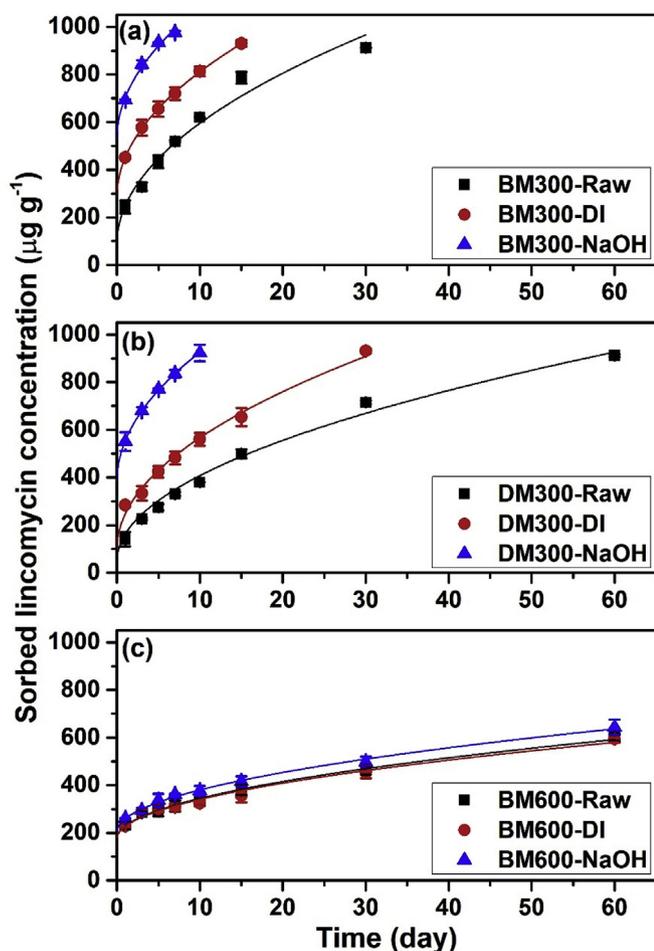
Fig. 4. Long-term kinetics of lincomycin sorption by raw-, DI-water-washed, and 0.01M-NaOH-washed biochars: (a) BM300, (b) DM300, and (c) BM600. The sorption data were fitted by intraparticle diffusion model (solid line). The symbols and error bars represent mean and standard deviation of duplicates.

Fig. S10), and the DOC removal with NaOH solution was more effective than that with DI water for the enhancement of sorption kinetics for BM300 and DM300 because a greater amount of DOC was removed (Fig. 4a and b). In addition, the fitted k_{id} and C_{id} values both increased after the DOC removal for these tested biochars (Table S6). For example, the k_{id} values were 160, 166 and 176 μg g $^{-1}$ day$^{-0.5}$ and the C_{id} values were 87.9, 285 and 527 μg g^{-1} for BM300-Raw, BM300-DI, and BM300-NaOH biochars, respectively. In contrast, the enhancement of lincomycin sorption kinetics by the DOC removal was very limited for BM600 due to its low DOC content (Fig. 4c). The above observations confirmed that the long-term release of DOC from biochars could increase their sorption ability for lincomycin, presumably because of increased accessibility to surface adsorption sites and pores initially blocked by biochar-DOC (Wang et al., 2017a). Furthermore, a close examination of SEM images revealed that the biochar particles of low-temperature biochars (e.g., BM300) were disintegrated, and the biochar particle size appeared to decrease after aging in 0.02 M background solution for 365-d and in 0.1 M NaOH solution for 1-d, presumably because of the DOC release from the biochars (Fig. S11). We further compared the size of biochar colloids by aging BM300 and BM600 biochars in either 0.1 M NaOH or 0.1 M NaCl solution (Fig. S12). The size of biochar colloids was much smaller in 0.1 M NaOH than in 0.1 M NaCl for BM300, whereas no obvious difference was observed for BM600. The decrease in particle size of BM300

after the DOC removal suggested that the surface sorption sites and pores initially located in deeper biochar pores could become accessible for lincomycin sorption after the breakdown of biochar particles, and thus further facilitated the sorption kinetics. Considering that BM600 was highly carbonized, and had a relatively low DOC content and rigid pore structure, the DOC removal would not substantially alter the surface sorption sites and pore structure of BM600, resulting in minimal enhancement of the sorption kinetics. In summary, these results supported the interpretation that the substantial release of biochar-DOC enhanced the long-term lincomycin sorption on biochars through increasing accessibility of sorption sites initially blocked by DOC as well as decreasing biochar particle sizes.

3.5. Extraction of sorbed-lincomycin from biochars

As shown in Fig. 5a, the extraction recoveries of lincomycin for all tested biochars were generally low and ranged from the lowest of 0.02% for BM300 to the highest of 24.7% for PM500. Thus, the long-term sorbed lincomycin on the biochars could be highly resistant to desorption. In addition, the extraction recoveries exhibited a negative logarithmic correlation with the k_{id} ($R^2 = 0.721$) (Fig. 5b), implying that faster pore diffusion would cause lower extraction recoveries. Furthermore, the results from an additional sorption/extraction experiment for DM600 biochar (described in Supplementary Material) revealed that the extraction recoveries decreased from $62.4 \pm 6.3\%$, $28.4 \pm 5.9\%$, to $8.75 \pm 0.47\%$ as sorption equilibration time increased from 1, 4, to 30 days (Fig. S13). These observations were presumably because lincomycin may diffuse deeper into the biochar pores and become trapped in the narrower pores by either faster diffusion rate or longer diffusion time, resulting in a lower extraction recovery. From the standpoint of soil biochar amendment for contaminant immobilization, the observed strong sorption and low extraction recovery for lincomycin may be desirable because the sorbed lincomycin would tend to remain within the biochars over the long term, thus reducing the mobility and bioavailability of lincomycin in soils.

4. Conclusions

This study demonstrated that the slow-pyrolysis biochars produced at 300–600 °C could strongly sequester lincomycin from water over the long-term. The long-term lincomycin sorption kinetics on the biochars were governed by fast surface sorption and slow intraparticle pore diffusion. Specially, the biochars produced at 300 and 600 °C generally exhibited faster lincomycin sorption kinetics than the biochars produced at 400–500 °C. The faster sorption kinetics for the biochars produced at 600 °C could be attributed to their greater specific surface area and pore volume, whereas for the biochars produced at 300 °C it was due to the long-term release of biochar-DOC. The substantial and continuous release of DOC from biochars could enhance the lincomycin sorption because of increased accessibility of sorption sites initially blocked by DOC on the external surface and in pore structure as well as decreased biochar particle sizes. The quasi-equilibrium sorption isotherms were more nonlinear for high-temperature biochars, due to the wider energy distribution of sorption sites on their surfaces. The sorption isotherms also became increasingly nonlinear with increasing equilibration time, likely resulting from the release of biochar-DOC. In addition, lincomycin sequestered in the biochars had a low extraction recovery presumably because lincomycin was strongly trapped within biochar pores.

We have previously proposed that sequestering antibiotics by biochars produced from animal manure may be a novel strategy for managing animal manures and manure-borne antibiotics (Liu et al.,
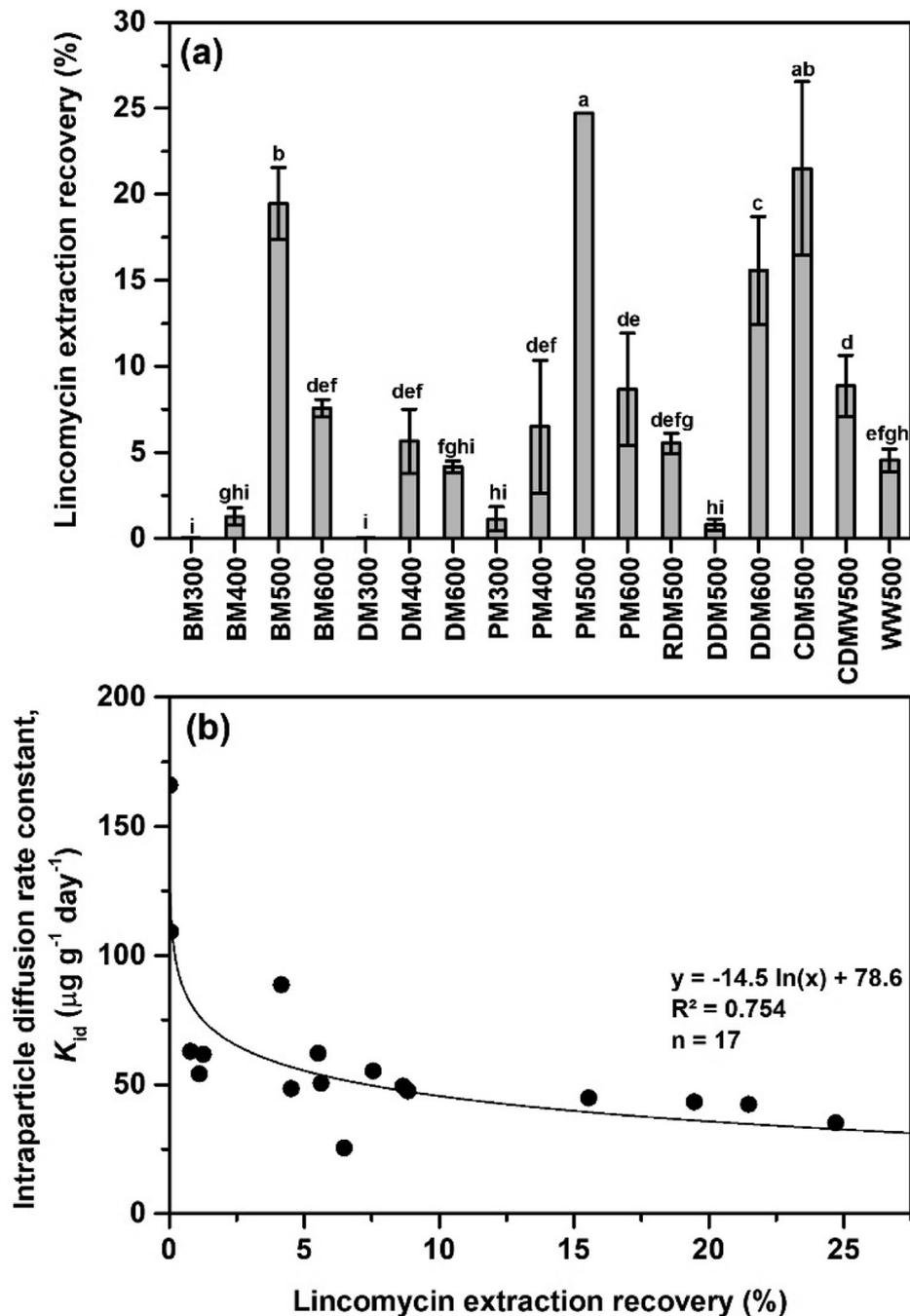
Fig. 5. (a) Extraction recovery of 240-d-sorbed lincomycin in the biochars and (b) the relationship of intraparticle diffusion rate constant (k_{id}) versus lincomycin extraction recovery for biochars.

2016). Using manure as feedstock to produce biochars could destroy any microbial pathogen and antibiotics via pyrolysis (i.e. 300—600 °C). The produced biochars could be applied in soils to reduce the mobility and bioavailability of anthropogenic antibiotics in water flows. Under the same tested concentration range (0—1000 $\mu g\,L^{-1}$), the observed K_d values of lincomycin (i.e., $C_w = 1\,\mu g\,L^{-1}$) on tested biochars after either 1 day (0.827—15.4 $L\,g^{-1}$) or 365 days (20.5—454 $L\,g^{-1}$) were greater than the previously reported K_d values for whole soils (0.00—0.476 $L\,g^{-1}$) (Wang et al., 2012). It should be noted that this study was limited to alkaline condition (pH 10), and is thus most relevant for alkaline soils. The release of DOC from biochars in alkaline soils via aging could

further enhance the sorption of antibiotics. Coupled with the strong irreversible sorption, biochars are a promising soil amendment for enhancing both short- and long-term sequestration of antibiotics and reducing the mobility and bioavailability of antibiotics in soils. Future studies should investigate contaminant sorption properties of biochars that are aged in a variety of soils of different pH.

Declaration of interests

The authors declare that they have no known competing financial interests or personal relationships that could have appeared to influence the work reported in this paper.

Appendix A. Supplementary data

Supplementary data to this article can be found online at https://doi.org/10.1016/j.watres.2019.06.006.

References

Ahmad, M., Rajapaksha, A.U., Lim, J.E., Zhang, M., Bolan, N., Mohan, D., Vithanage, M., Lee, S.S., Ok, Y.S., 2014. Biochar as a sorbent for contaminant management in soil and water: a review. Chemosphere 99, 19—33.

Ahmed, M.B., Zhou, J.L., Ngo, H.H., Guo, W., 2015. Adsorptive removal of antibiotics from water and wastewater: progress and challenges. Sci. Total Environ. 532, 112—126.

Andreozzi, R., Canterino, M., Lo Giudice, R., Marotta, R., Pinto, G., Pollio, A., 2006. Lincomycin solar photodegradation, algal toxicity and removal from wastewaters by means of ozonation. Water Res. 40 (3), 630—638.

Antal, M.J., Gronli, M., 2003. The art, science, and technology of charcoal production. Ind. Eng. Chem. Res. 42 (8), 1619—1640.

Beesley, L., Moreno-Jimenez, E., Gomez-Eyles, J.L., Harris, E., Robinson, B., Sizmur, T., 2011. A review of biochars' potential role in the remediation, revegetation and restoration of contaminated soils. Environ. Pollut. 159 (12), 3269—3282.

Bernal, M.P., Alburquerque, J.A., Moral, R., 2009. Composting of animal manures and chemical criteria for compost maturity assessment. A review. Bioresour. Technol. 100 (22), 5444—5453.

Calza, P., Medana, C., Padovano, E., Dal Bello, F., Baiocchi, C., 2012. Identification of the unknown transformation products derived from lincomycin using LC-HRMS technique. J. Mass Spectrom. 47 (6), 751—759.

Chee-Sanford, J.C., Mackie, R.I., Koike, S., Krapac, I.G., Lin, Y.F., Yannarell, A.C., Maxwell, S., Aminov, R.I., 2009. Fate and transport of antibiotic residues and antibiotic resistance genes following land application of manure waste. J. Environ. Qual. 38 (3), 1086—1108.

Chen, B., Zhou, D., Zhu, L., 2008. Transitional adsorption and partition of nonpolar and polar aromatic contaminants by biochars of pine needles with different pyrolytic temperatures. Environ. Sci. Technol. 42 (14), 5137—5143.

Chen, Z., Chen, B., Chiou, C.T., 2012. Fast and slow rates of naphthalene sorption to biochars produced at different temperatures. Environ. Sci. Technol. 46 (20), 11104—11111.

Chuang, Y.H., Zhang, Y., Zhang, W., Boyd, S.A., Li, H., 2015. Comparison of accelerated solvent extraction and quick, easy, cheap, effective, rugged and safe method for extraction and determination of pharmaceuticals in vegetables. J. Chromatogr. A 1404, 1—9.

Chun, Y., Sheng, G., Chiou, C.T., Xing, B., 2004. Compositions and sorptive properties of crop residue-derived chars. Environ. Sci. Technol. 38 (17), 4649—4655.

De Haan, H., De Boer, T., 1987. Applicability of light absorbance and fluorescence as measures of concentration and molecular size of dissolved organic carbon in humic Lake Tjeukemeer. Water Res. 21 (6), 731—734.

Ding, Y., Teppen, B.J., Boyd, S.A., Li, H., 2013. Measurement of associations of pharmaceuticals with dissolved humic substances using solid phase extraction. Chemosphere 91 (3), 314—319.

Enders, A., Hanley, K., Whitman, T., Joseph, S., Lehmann, J., 2012. Characterization of biochars to evaluate recalcitrance and agronomic performance. Bioresour. Technol. 114, 644—653.

Feng, D., Yu, H.M., Deng, H., Li, F.Z., Ge, C.J., 2015. Adsorption characteristics of norfloxacin by biochar prepared by cassava dreg: kinetics, isotherms, and thermodynamic analysis. BioResources 10 (4), 6751—6768.

Heuer, H., Schmitt, H., Smalla, K., 2011. Antibiotic resistance gene spread due to manure application on agricultural fields. Curr. Opin. Microbiol. 14 (3), 236—243.

Huang, H., Tang, J.C., Gao, K., He, R.Z., Zhao, H., Werner, D., 2017. Characterization of KOH modified biochars from different pyrolysis temperatures and enhanced adsorption of antibiotics. RSC Adv. 7 (24), 14640—14648.

IBI, 2019. Standardized product definition and product testing guidelines for biochar that is used in soil (aka IBI biochar standards) version 2.1. http://www.biochar-international.org/characterizationstandard. (Accessed 15 May 2019).

Kah, M., Sigmund, G., Xiao, F., Hofmann, T., 2017. Sorption of ionizable and ionic organic compounds to biochar, activated carbon and other carbonaceous materials. Water Res. 124, 673—692.

Kasozi, G.N., Zimmerman, A.R., Nkedi-Kizza, P., Gao, B., 2010. Catechol and humic acid sorption onto a range of laboratory-produced black carbons (biochars). Environ. Sci. Technol. 44 (16), 6189—6195.

Keiluweit, M., Nico, P.S., Johnson, M.G., Kleber, M., 2010. Dynamic molecular structure of plant biomass-derived black carbon (biochar). Environ. Sci. Technol. 44 (4), 1247—1253.

Kolpin, D.W., Furlong, E.T., Meyer, M.T., Thurman, E.M., Zaugg, S.D., Barber, L.B., Buxton, H.T., 2002. Pharmaceuticals, hormones, and other organic wastewater contaminants in US streams, 1999-2000: a national reconnaissance. Environ. Sci. Technol. 36 (6), 1202—1211.

Kuchta, S.L., Cessna, A.J., 2009. Fate of lincomycin in snowmelt runoff from manure-amended pasture. Chemosphere 76 (4), 439—446.

Kumar, K., Gupta, S.C., Chander, Y., Singh, A.K., 2005. Antibiotic use in agriculture and its impact on the terrestrial environment. Adv. Agron. 87 87, 1—54.

Kummerer, K., 2009. Antibiotics in the aquatic environment — a review — Part I. Chemosphere 75 (4), 417—434.

Lehmann, J., 2007. Bio-energy in the black. Front. Ecol. Environ. 5 (7), 381—387.

Lehmann, J., Joseph, S., 2015. Biochar for Environmental Management: Science, Technology and Implementation. Routledge.

Lian, F., Sun, B., Song, Z., Zhu, L., Qi, X., Xing, B., 2014. Physicochemical properties of herb-residue biochar and its sorption to ionizable antibiotic sulfamethoxazole. Chem. Eng. J. 248, 128—134.

Lian, F., Xing, B., 2017. Black carbon (biochar) in water/soil environments: molecular structure, sorption, stability, and potential risk. Environ. Sci. Technol. 51 (23), 13517—13532.

Lin, Y., Munroe, P., Joseph, S., Henderson, R., Ziolkowski, A., 2012. Water extractable organic carbon in untreated and chemical treated biochars. Chemosphere 87 (2), 151—157.

Liu, C.H., Chu, W.Y., Li, H., Boyd, S.A., Teppen, B.J., Mao, J.D., Lehmann, J., Zhang, W., 2019. Quantification and characterization of dissolved organic carbon from biochars. Geoderma 335, 161—169.

Liu, C.H., Chuang, Y.H., Li, H., Teppen, B.J., Boyd, S.A., Gonzalez, J.M., Johnston, C.T., Lehmann, J., Zhang, W., 2016. Sorption of lincomycin by manure-derived biochars from water. J. Environ. Qual. 45 (2), 519—527.

Loftin, K.A., Adams, C.D., Meyer, M.T., Surampalli, R., 2008. Effects of ionic strength, temperature, and pH on degradation of selected antibiotics. J. Environ. Qual. 37 (2), 378—386.

Martinez, J.L., 2009. Environmental pollution by antibiotics and by antibiotic resistance determinants. Environ. Pollut. 157 (11), 2893—2902.

Mukherjee, A., Zimmerman, A.R., 2013. Organic carbon and nutrient release from a range of laboratory-produced biochars and biochar—soil mixtures. Geoderma 193—194, 122—130.

Pan, B., Huang, P., Wu, M., Wang, Z., Wang, P., Jiao, X., Xing, B., 2012. Physicochemical and sorption properties of thermally-treated sediments with high organic matter content. Bioresour. Technol. 103 (1), 367—373.

Peiris, C., Gunatilake, S.R., Mlsna, T.E., Mohan, D., Vithanage, M., 2017. Biochar based removal of antibiotic sulfonamides and tetracyclines in aquatic environments: a critical review. Bioresour. Technol. 246, 150—159.

Pignatello, J.J., 2013. Adsorption of dissolved organic compounds by black carbon. In: Xu, J., Sparks, L.D. (Eds.), Molecular Environmental Soil Science. Springer Netherlands, Dordrecht, pp. 359—385.

Qu, X.L., Fu, H.Y., Mao, J.D., Ran, Y., Zhang, D.N., Zhu, D.Q., 2016. Chemical and structural properties of dissolved black carbon released from biochars. Carbon 96, 759—767.

Rajkovich, S., Enders, A., Hanley, K., Hyland, C., Zimmerman, A.R., Lehmann, J., 2011. Corn growth and nitrogen nutrition after additions of biochars with varying properties to a temperate soil. Biol. Fertil. Soils 48 (3), 271—284.

Rivera-Utrilla, J., Sanchez-Polo, M., Ferro-Garcia, M.A., Prados-Joya, G., Ocampo-Perez, R., 2013. Pharmaceuticals as emerging contaminants and their removal from water. A review. Chemosphere 93 (7), 1268—1287.

Sarmah, A.K., Meyer, M.T., Boxall, A.B., 2006. A global perspective on the use, sales, exposure pathways, occurrence, fate and effects of veterinary antibiotics (VAs) in the environment. Chemosphere 65 (5), 725—759.

Shang, J.G., Kong, X.R., He, L.L., Li, W.H., Liao, Q.J.H., 2016. Low-cost biochar derived from herbal residue: characterization and application for ciprofloxacin adsorption. Int. J. Environ. Sci. Technol. 13 (10), 2449—2458.

Sigmund, G., Huffer, T., Hofmann, T., Kah, M., 2017. Biochar total surface area and total pore volume determined by N_2 and CO_2 physisorption are strongly influenced by degassing temperature. Sci. Total Environ. 580, 770—775.

Sim, W.J., Lee, J.W., Lee, E.S., Shin, S.K., Hwang, S.R., Oh, J.E., 2011. Occurrence and distribution of pharmaceuticals in wastewater from households, livestock farms, hospitals and pharmaceutical manufactures. Chemosphere 82 (2), 179—186.

Smith, C.R., Hatcher, P.G., Kumar, S., Lee, J.W., 2016. Investigation into the sources of biochar water-soluble organic compounds and their potential toxicity on aquatic microorganisms. ACS Sustain. Chem. Eng. 4 (5), 2550—2558.

Sposito, G., 1980. Derivation of the Freundlich equation for ion exchange reactions in Soils1. Soil Sci. Soc. Am. J. 44 (3), 652—654.

Tan, X., Liu, Y., Zeng, G., Wang, X., Hu, X., Gu, Y., Yang, Z., 2015. Application of biochar for the removal of pollutants from aqueous solutions. Chemosphere 125, 70—85.

Uyguner, C.S., Bekbolet, M., 2005. Implementation of spectroscopic parameters for practical monitoring of natural organic matter. Desalination 176 (1—3), 47—55.

Van Boeckel, T.P., Glennon, E.E., Chen, D., Gilbert, M., Robinson, T.P., Grenfell, B.T., Levin, S.A., Bonhoeffer, S., Laxminarayan, R., 2017. Reducing antimicrobial use in food animals. Science 357 (6358), 1350—1352.

Van Epps, A., Blaney, L., 2016. Antibiotic residues in animal waste: occurrence and degradation in conventional agricultural waste management practices. Current Pollution Reports 2 (3), 135—155.

Wang, B., Zhang, W., Li, H., Fu, H., Qu, X., Zhu, D., 2017a. Micropore clogging by leachable pyrogenic organic carbon: a new perspective on sorption

irreversibility and kinetics of hydrophobic organic contaminants to black carbon. Environ. Pollut. 220 (Pt B), 1349–1358.

Wang, C.P., Teppen, B.J., Boyd, S.A., Li, H., 2012. Sorption of lincomycin at low concentrations from water by soils. Soil Sci. Soc. Am. J. 76 (4), 1222–1228.

Wang, H., Chu, Y., Fang, C., Huang, F., Song, Y., Xue, X., 2017b. Sorption of tetracycline on biochar derived from rice straw under different temperatures. PLoS One 12 (8), e0182776.

Watanabe, N., Bergamaschi, B.A., Loftin, K.A., Meyer, M.T., Harter, T., 2010. Use and environmental occurrence of antibiotics in freestall dairy farms with manured forage fields. Environ. Sci. Technol. 44 (17), 6591–6600.

Weber, W.J., Morris, J.C., 1963. Kinetics of adsorption on carbon from solution. J. Sanit. Eng. Div. 89 (2), 31–60.

Wu, F.C., Tseng, R.L., Juang, R.S., 2001. Kinetic modeling of liquid-phase adsorption of reactive dyes and metal ions on chitosan. Water Res. 35 (3), 613–618.

Wu, F.C., Tseng, R.L., Juang, R.S., 2009. Initial behavior of intraparticle diffusion model used in the description of adsorption kinetics. Chem. Eng. J. 153 (1–3), 1–8.

Wu, M., Pan, B., Zhang, D., Xiao, D., Li, H., Wang, C., Ning, P., 2013. The sorption of organic contaminants on biochars derived from sediments with high organic carbon content. Chemosphere 90 (2), 782–788.

Xing, B.S., Pignatello, J.J., 1996. Time-dependent isotherm shape of organic compounds in soil organic matter: implications for sorption mechanism. Environ. Toxicol. Chem. 15 (8), 1282–1288.

Zhang, G., Zhang, Q., Sun, K., Liu, X., Zheng, W., Zhao, Y., 2011. Sorption of simazine to corn straw biochars prepared at different pyrolytic temperatures. Environ. Pollut. 159 (10), 2594–2601.

Zhang, M., Liu, Y.S., Zhao, J.L., Liu, W.R., He, L.Y., Zhang, J.N., Chen, J., He, L.K., Zhang, Q.Q., Ying, G.G., 2018. Occurrence, fate and mass loadings of antibiotics in two swine wastewater treatment systems. Sci. Total Environ. 639, 1421–1431.

Zhang, Q.Q., Ying, G.G., Pan, C.G., Liu, Y.S., Zhao, J.L., 2015. Comprehensive evaluation of antibiotics emission and fate in the river basins of China: source analysis, multimedia modeling, and linkage to bacterial resistance. Environ. Sci. Technol. 49 (11), 6772–6782.

Zheng, H., Wang, Z.Y., Zhao, J., Herbert, S., Xing, B.S., 2013. Sorption of antibiotic sulfamethoxazole varies with biochars produced at different temperatures. Environ. Pollut. 181, 60–67.

Zhu, Y.G., Johnson, T.A., Su, J.Q., Qiao, M., Guo, G.X., Stedtfeld, R.D., Hashsham, S.A., Tiedje, J.M., 2013. Diverse and abundant antibiotic resistance genes in Chinese swine farms. Proc. Natl. Acad. Sci. U. S. A. 110 (9), 3435–3440.

Zimmerman, A.R., Gao, B., 2013. In: Ladygina, N., Rineau, F. (Eds.), The Stability of Biochar in the Environment. Biochar and Soil Biota. CRC Press, pp. 1–40.